

Third-order nonlinear optical spectroscopy in the two-dimensional cuprates Nd_2CuO_4 and La_2CuO_4

H. Kishida,^{1,2} M. Ono,¹ A. Sawa,³ M. Kawasaki,^{3,4} Y. Tokura,^{3,5} and H. Okamoto^{1,3}

¹*Department of Advanced Materials Science, Graduate School of Frontier Sciences, University of Tokyo, Kashiwa, Chiba 277-8561, Japan*

²*Structural Ordering and Physical Properties Group, Precursory Research for Embryonic Science and Technology (PRESTO), Japan Science and Technology Corporation (JST), Kashiwa 277-8561, Japan*

³*Correlated Electron Research Center (CERC), National Institute of Advanced Industrial Science and Technology (AIST), Tsukuba, 305-8562, Japan*

⁴*Institute for Materials Research, Tohoku University, Sendai 980-8577, Japan*

⁵*Department of Applied Physics, University of Tokyo, Tokyo 113-8656, Japan*

(Received 10 January 2003; published 4 August 2003)

We have measured third-order nonlinear susceptibility ($\chi^{(3)}$) spectra of the two-dimensional (2D) cuprates La_2CuO_4 and Nd_2CuO_4 by third-harmonic generation. The $|\chi^{(3)}|$ spectra exhibit broad peaks with maximum values of 0.6×10^{-10} esu in La_2CuO_4 and 2×10^{-10} esu in Nd_2CuO_4 . These peaks are attributable to three-photon resonance to the charge transfer (CT) excited state. The $\chi^{(3)}$ phase spectrum of Nd_2CuO_4 has revealed that the two-photon resonance to the even CT state are hidden on the high-energy side of the $\chi^{(3)}$ peak. The difference in $\chi^{(3)}$ values between the 2D and 1D cuprates is discussed by considering differences in spin-charge coupling and in charge configurations between the 2D and 1D cases.

DOI: 10.1103/PhysRevB.68.075101

PACS number(s): 78.66.Nk, 42.65.Ky

Nonlinear optical materials with large third-order nonlinear susceptibilities $\chi^{(3)}$ are indispensable in the creation of all-optical switching, modulating, and computing devices. Recently, electroreflectance (ER) and the third-harmonic generation (THG) spectroscopy results have shown that $\chi^{(3)}$ is anomalously enhanced in the one-dimensional (1D) Mott insulators (MIs) of CuO chains (Sr_2CuO_3 and Ca_2CuO_3) and NiX chains [halogen(X)-bridged Ni^{3+} compounds].^{1,2} In these materials, the Mott-Hubbard gap opens in the d band of copper (or nickel), due to large on-site Coulomb interactions U at metal sites and the occupied p band of oxygen (or halogen) located between the upper and lower Hubbard bands of the metal. Optical response is therefore dominated by charge transfer (CT) transitions from oxygen (or halogen) to copper (or nickel) with an energy of 1–2 eV.

The ER study on single-crystal samples of CuO and NiX chains revealed that $\chi^{(3)}(-\omega; 0, 0, \omega)$, defined by $P(\omega) = 3\epsilon_0\chi^{(3)}(-\omega; 0, 0, \omega)E(0)^2E(\omega)$, reaches 10^{-8} to 10^{-5} esu, where $P(\omega)$ represents nonlinear polarization, $E(0)$ is the static electric field, $E(\omega)$ is the electric field of light, and ϵ_0 is the permittivity of free space. Analysis of $\chi^{(3)}(-\omega; 0, 0, \omega)$ spectra, based on a simple three-level model, has suggested that the odd and even CT states are nearly degenerate and that the enhancement of $\chi^{(3)}$ is due to a large transition dipole moment between the two states. Degeneracy of the odd and even CT states has also been demonstrated by two-photon absorption measurements of Sr_2CuO_3 .^{3,4} The THG studies of single crystalline CuO chain thin films have shown that $\chi^{(3)}(-3\omega; \omega, \omega, \omega)$, defined as $P(3\omega) = 1/4\epsilon_0\chi^{(3)}(-3\omega; \omega, \omega, \omega)E(\omega)^3$, is also very large (10^{-10} to 10^{-9} esu) and that the shapes of spectra of such films are well explained by assuming the presence of nearly degenerate odd and even CT states.²

Recent theoretical studies suggest that such degeneracy of CT states and enhancement of dipole moment are character-

istic of the 1D MIs and do not necessarily hold for the 2D MIs.^{5,6} For an overall understanding of the nonlinear optical response in correlated electron systems, it is necessary to investigate $\chi^{(3)}$ spectra of the 2D MIs. So far, $\chi^{(3)}(-3\omega; \omega, \omega, \omega)$ spectra of the 2D Mott insulators have been reported for La_2CuO_4 and $\text{Sr}_2\text{CuO}_2\text{Cl}_2$ by Schülzgen *et al.*⁷ and Schumacher *et al.*⁸, respectively. Spectral shapes of $\chi^{(3)}(-3\omega; \omega, \omega, \omega)$ in the two reports are conspicuously different. The THG spectrum of La_2CuO_4 consists of several peaks, which have been attributed to quantum interference from three-photon resonance to the CT states with E_u symmetry and two-photon resonance to the CT states with A_{1g} , A_{2g} , and B_{1g} symmetries. The THG spectrum of $\text{Sr}_2\text{CuO}_2\text{Cl}_2$, however, exhibits only a single broad peak. Schumacher *et al.* have asserted that this resonant structure is mainly due to the three-photon resonance of the CT states with E_u symmetry. They also suggest that interference between two intermediate states with even parity, an A_{1g} excited state and the B_{1g} ground state, influences the spectral shape of $\chi^{(3)}$. In the former study, absolute values of $\chi^{(3)}$ were not determined, whereas in the latter study, absolute values of $\chi^{(3)}$ were determined, while the measured spectral range was limited. Thus, lack of experimental information makes complete interpretation of third-order nonlinear optical response of the 2D cuprates difficult.

We report quantitative analysis of full $|\chi^{(3)}(-3\omega; \omega, \omega, \omega)|$ spectra of the 2D MIs La_2CuO_4 and Nd_2CuO_4 , by the THG in single crystalline thin-film samples. Because resonant structures of the obtained $\chi^{(3)}$ spectra are quite broad, it is difficult to deduce electronic configurations of the 2D MIs directly from spectral envelopes alone. Therefore, phase (ϕ) spectra of $\chi^{(3)}(-3\omega; \omega, \omega, \omega) = |\chi^{(3)}|\exp(i\phi)$, which directly reflect energy-level structures, were measured. Dimensionality dependence of nonlinear optical response in MIs is examined by comparing results with those of the 1D MIs.

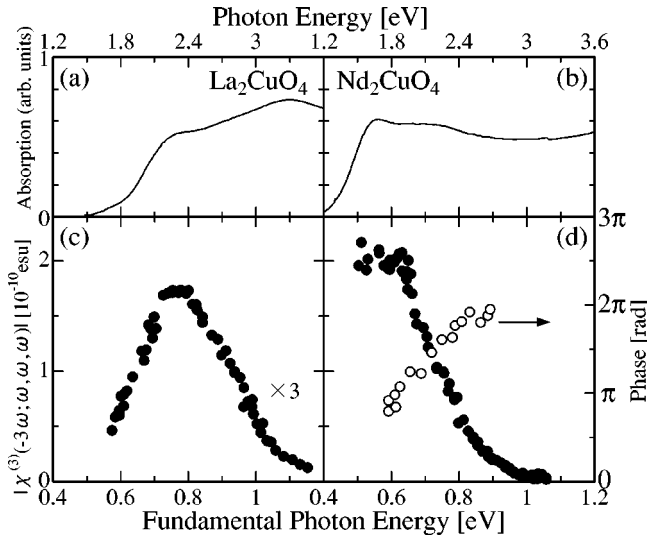


FIG. 1. Absorption spectra of (a) La_2CuO_4 and (b) Nd_2CuO_4 thin films. $|\chi^{(3)}(-3\omega; \omega, \omega, \omega)|$ spectra of La_2CuO_4 and Nd_2CuO_4 are shown in (c) and (d), respectively, by filled circles. Open circles in (d) show the $\chi^{(3)}(-3\omega; \omega, \omega, \omega)$ phase spectrum of Nd_2CuO_4 .

Thin films were deposited by laser molecular beam epitaxy, with La_2CuO_4 deposited onto $\text{LaSrAlO}_4(001)$ substrate and Nd_2CuO_4 deposited onto $[\text{LaAlO}_3]_{0.3} + [\text{Sr}_2\text{AlTaO}_6]_{0.7}$ substrate. For $|\chi^{(3)}|$ measurement, 1550-Å thick La_2CuO_4 and 1200-Å thick Nd_2CuO_4 were used, while for phase spectrum measurement 150–2000-Å thick Nd_2CuO_4 films were used. In THG experiments, 6 ns light pulses produced by a Q switched Nd:YAG laser and tunable optical parametric oscillator were used. To determine the absolute value of $\chi^{(3)}$, Maker's fringe patterns were measured and the THG intensity of the thin films was compared with that of a SiO_2 reference sample.⁹ The SiO_2 $\chi^{(3)}$ spectrum was calculated by applying Miller's rule^{10,11} to the reported $\chi^{(3)}$ value of 1.907 μm .¹² To avoid experimental errors due to the THG of ambient air from being included in results, all measurements were performed in a vacuum.⁹ $\chi^{(3)}$ values of the samples were calculated using Eq. (1):

$$|\chi_f^{(3)}| = |\chi_r^{(3)}| \frac{2}{\pi} \frac{l_c}{d_f} \sqrt{\frac{I_f}{I_r}} \frac{\alpha_f d_f / 2}{1 - \exp(-\alpha_f d_f / 2)}, \quad (1)$$

where l_c is the coherence length of SiO_2 , d_f is film thickness of the sample, I_f is the THG intensity of the sample, and I_r is the THG intensity of the SiO_2 reference. Note that the absorption (α_f) of the third-harmonic (TH) light within the thin films has been taken into account. $\chi^{(3)}$ phase ϕ is measured from interference between the TH light from the sample and from the substrate. Therefore, proper film thickness is needed to be chosen, depending on the incident light wavelength, so that the THG intensity from the film would be comparable to that from the substrate. Details of the experimental technique have been reported previously.¹³

Absorption spectra of La_2CuO_4 and Nd_2CuO_4 thin films are presented in Figs. 1(a) and (b), respectively. Absorption peaks are located at around 2.22 eV in La_2CuO_4 and 1.60 eV in Nd_2CuO_4 . These peaks are attributable to the CT transi-

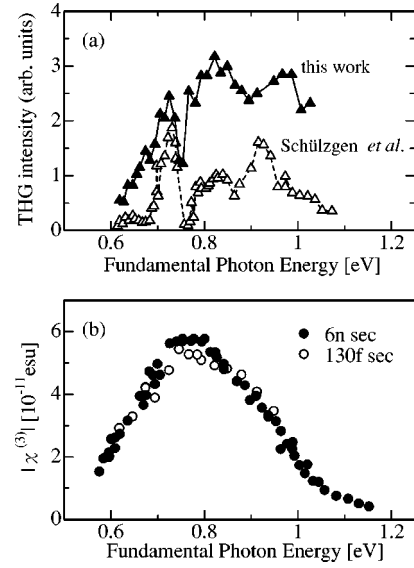


FIG. 2. (a) Spectrum of the third-harmonic generation intensity in La_2CuO_4 under constant incident power (0.3 μJ) (filled triangles). Open triangles show the results of Schülzgen *et al.*⁷ (b) Comparison of $\chi^{(3)}$ spectra obtained using femtosecond laser pulses (open circles) and nanosecond laser pulses (filled circles).

tions from oxygen to Cu.¹⁴ $|\chi^{(3)}(-3\omega; \omega, \omega, \omega)|$ spectra are shown by filled circles in the Figs. 1(c) and (d). Peaks are observed at 0.78 eV in La_2CuO_4 and 0.55 eV in Nd_2CuO_4 . Because these energies are equal to the one third of the CT transition energy, the peaks can be attributed to three-photon resonance to the CT excited state. Absolute values around the resonant peaks are 0.6×10^{-10} esu for La_2CuO_4 and 2×10^{-10} esu for Nd_2CuO_4 .

The measured $\chi^{(3)}$ spectrum of La_2CuO_4 only exhibits a single broad peak, in contrast with the results previously reported by Schülzgen *et al.*, which exhibited pronounced peaks at 0.65, 0.72, 0.79, 0.84, 0.92, and 1 eV, as shown in Fig. 2(a) by open triangles. Since sample preparation and linear absorption spectra were essentially the same, differences in $\chi^{(3)}$ measurement methods are thought to have been responsible for $\chi^{(3)}$ spectral differences. In particular, THG intensity was measured by Schülzgen using femtosecond laser pulses, a reference sample was not used, and incident power was kept constant at 3 μJ during THG intensity measurement. To isolate the source of differences in the results, we performed experiments following the procedures used by Schülzgen *et al.*

The THG spectra were measured using 130 fs laser pulses from a Ti-sapphire (Ti-S) regenerative amplifier (Spectra Physics, Hurricane) and optical parametric amplifier (OPA) (Quantronics, TOPAS). Incident light was normal to the sample, with intensity fixed at 0.3 μJ . Figure 2(a) shows the obtained THG spectrum as filled triangles, exhibiting a sharp dip at around 0.77 eV, which can also be seen in the Schülzgen *et al.* spectrum (open triangles). The overall spectral shapes are quite similar. Next, the THG intensity of the sample was compared with that of the reference (SiO_2) by means of Maker's fringes. The $\chi^{(3)}$ spectrum, calculated using Eq. (1), is shown in Fig. 2(b), by open circles. The $\chi^{(3)}$

spectrum resulting from nanosecond laser pulses is shown for comparison by filled circles. The two $\chi^{(3)}$ spectra are almost identical in terms of both magnitude and spectral shape. Thus, it is clear that sharp features in the THG spectrum reported by Schülzgen *et al.* are experimental artifacts. The dip observed at 0.775 eV [Fig. 2(a)] corresponds to the degenerating point of the Ti-S-laser-based OPA, where signal and idler beam photon energies match. At this point, electric-field amplitude usually decreases due to elongation of the pulse width, thus suppressing THG intensity. The presented results verify that such an experimental problem can be avoided by using a reference sample.

We now turn our attention to the physical mechanisms of the nonlinear optical response in 2D cuprates. For this, it is useful to analyze, phenomenologically, the $\chi^{(3)}$ spectrum, assuming a discrete energy-level model. Generally, the THG processes that resonate with the optical gap can be classified into either one of the two categories shown in Fig. 3. G , A , and X denote the ground state, a one-photon allowed state,

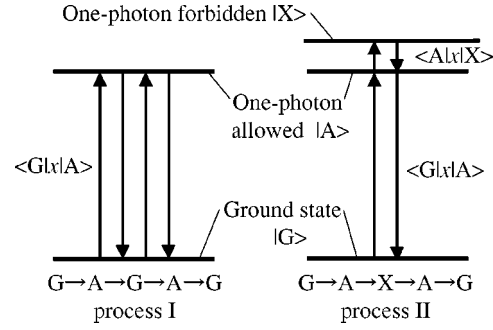


FIG. 3. Two types of third-order nonlinear optical processes. Process I consists of the ground state (G) and a one-photon allowed state (A). In process II, an additional one-photon forbidden excited state (X) also contributes to the process.

and a one-photon forbidden state, respectively. Process I involves only two of the states, G and X , while process II involves all three states G , A , and X . In both processes, the main term describing THG resonance is given by Eq. (2):¹⁵

$$\chi^{(3)}(-3\omega; \omega, \omega, \omega)_{\text{main}} = \frac{Ne^4}{\epsilon_0 \hbar^3} \frac{\langle G|x|A\rangle \langle A|x|m\rangle \langle m|x|A\rangle \langle A|x|G\rangle}{(\omega_A - 3\omega - i\gamma_A)(\omega_m - 2\omega - i\gamma_m)(\omega_A - \omega - i\gamma_A)}, \quad (2)$$

where N is the number of Cu sites per unit volume and $\omega_{A,m}$ and $\gamma_{A,m}$ are the energy and damping factor of state A and another intermediate state m ($=X$ or G), respectively. Transition dipole moment $\langle G|x|A\rangle$ can be calculated from the linear absorption spectra (ϵ_2). Values of $\langle G|x|A\rangle$ obtained for La_2CuO_4 and Nd_2CuO_4 were 0.30 Å and 0.46 Å, respectively. Using these values, resonant $\chi^{(3)}$ of process I was calculated to be 10^{-13} esu, two orders of magnitudes smaller than the experimental values. This suggests that the intermediate state contributing to $\chi^{(3)}$ is not the ground state (process I), but the one-photon forbidden excited state of process II.

Direct evidence of the one-photon forbidden excited state contributing to $\chi^{(3)}$ can be obtained from the phase spectra of $\chi^{(3)}(-3\omega; \omega, \omega, \omega)$. The energy denominator of Eq. (2) describes three resonant processes, which occur at $\omega = 1/3\omega_A$ (three-photon resonance), $\omega = 1/2\omega_m$ (two-photon resonance), and $\omega = \omega_A$ (one-photon resonance). At each resonant energy the sign of the energy denominator changes and thus the phase of $\chi^{(3)}$ changes by π . In process I, the phase spectrum starts at π , even in the lower-energy side, and then changes from π to 2π across the three-photon resonance. In process II, however, the phase changes from 0 to π across the three-photon resonance and from π to 2π across the two-photon resonance.

The phase spectrum obtained for Nd_2CuO_4 is shown in Fig. 1(d) by open circles. Phase gradually increases with energy from 0.6π at 0.6 eV to 2π at 0.9 eV. Since phase is initially less than π and is still only π at the three-photon resonant peak, process I can be ruled out as a major contribu-

tor. The phase changes from π to 2π at around 0.75 eV and saturates at about 0.9 eV, indicating that two-photon resonance occurs at around 0.75 eV. Namely, the one-photon forbidden state with even parity is located around 1.5 eV, which will also be attributable to the CT excited states, judging from the energy position.

By fitting discrete-level model calculations to experimental $|\chi^{(3)}|$ spectra, energies of the one-photon forbidden level and transition dipole moments can be estimated. Values of $\omega_X = 1.80$ eV (1.43 eV) and $\langle A|x|X\rangle = 8.5$ Å (6.4 Å) were obtained for La_2CuO_4 (Nd_2CuO_4). The energy level (1.43 eV) of X for Nd_2CuO_4 is consistent with phase spectrum results. This indicates that state X is the even CT state located near the odd CT state. Furthermore, since $\langle A|x|X\rangle$ was found to be much larger than $\langle G|x|A\rangle$, we can conclude that the large value of $\langle A|x|X\rangle$ is responsible for the enhanced $\chi^{(3)}$. This is a mechanism similar to the one observed in the 1D MIs.¹

The three-level model discussed above is a useful tool for understanding overall spectral shapes. It is, however, reasonable to consider that photoexcited states of the 2D cuprates do not have discrete-level structures, as suggested by the previous studies.^{16,17} For example, the excitation profile of photoconductivity in La_2CuO_4 shows a threshold energy smaller than the ϵ_2 peak energy.¹⁶ This indicates that the lowest CT transition is not associated with an excitonic bound state but with electron-hole continuum. A theoretical model with the strong-coupling limit of a half-filled Hubbard model, which is thought to work well for the 2D cuprates has predicted continuum excited states around the CT gap

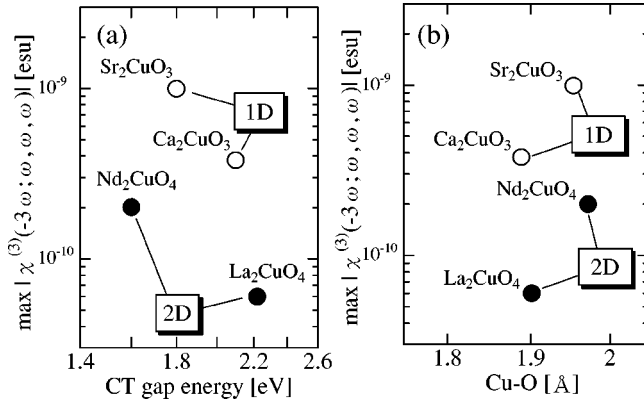


FIG. 4. (a) $\chi^{(3)}$ of the 1D and 2D cuprates as a function of the CT gap energy. (b) $\chi^{(3)}$ as a function of Cu-O length.

energy.⁶ The nonlinear susceptibility and phase spectra were also calculated based on this model. The result shows that the $\chi^{(3)}$ spectrum is dominated by the process of three-photon resonance associated with the odd CT states and that the contribution of the two-photon resonance to the even CT state is not observed as peak structures. However, the phase of $\chi^{(3)}$ reaches $3/2\pi$ near the two-photon resonance energy, indicating the significant contribution of two-photon resonance. These calculations are qualitatively consistent with both experimental spectra and results drawn from the simple three-level model.

It is worthwhile comparing the magnitudes of $\chi^{(3)}$ of the 2D cuprates and the 1D ones (Sr₂CuO₃ and Ca₂CuO₃). Maximum values of $\chi^{(3)}$ are plotted as a function of the CT gap energy in Fig. 4(a). With increasing CT gap energy, $\chi^{(3)}$ decreases in both 1D and 2D systems. To examine the dimensionality dependence of $\chi^{(3)}$, the CT gap-energy dependence of $\chi^{(3)}$ also needs to be considered. Figure 4(a) makes a direct comparison between the 1D and 2D systems possible. When compared at the same gap energy, $\chi^{(3)}$ values of 2D systems are approximately one order of magnitude smaller than those of 1D systems. This can be explained by enhancement of $\chi^{(3)}$ in 1D systems due to spin-charge separation.⁵ In 1D strongly correlated electron systems, charge and spin degrees of freedom are separated. As a result, optical excited states can be described as excited charged particles, having a doubly occupied state called a doublon and an empty state called a holon. The assumption of strong correlation between electrons prohibits a holon and a doublon from occupying the same site. In this case, odd and even states are always degenerate. Electron wave functions of the pair of odd and even states have a node at the origin of relative coordinates and show the same profile except for sign. This leads to an increase in transition dipole moment. However, in 2D systems, optical and charge excitations do not separate from spin excitations. Consequently, spatial overlap of electron wave functions between odd and even states is reduced. As a result, transition dipole moment, and therefore nonlinear susceptibility, are decreased. Our experimental results reflect such differences in dimensionality and capture spin-charge separation effects via nonlinear optical processes.

A different theoretical approach, based on the two-band Hubbard model, also gives reasons for $\chi^{(3)}$ being smaller in the 2D systems than in the 1D systems.¹⁸ In these calculations, larger $\chi^{(3)}$ in the 1D systems is also attributed to larger transition dipole moments between odd and even excited states. The reasoning is that in the 1D system, the two CT excitations, which are parallel and antiparallel to the chain, are degenerate. The one-photon allowed odd excited states and one-photon forbidden even ones correspond to asymmetric and symmetric combinations of the two CT configurations, respectively. In the 2D systems, on the other hand, one copper atom is surrounded by four equivalent oxygen atoms and thus four CT configurations from oxygen to copper exist. The one-photon allowed state is a combination of only two of these four configurations, while the one-photon forbidden state is a combination of all four. As a result, transition dipole moments between the one-photon allowed CT excited state and one-photon forbidden state are reduced. This explanation of the smaller $\chi^{(3)}$ in 2D will be verified by the investigation of the cross-polarized nonlinear optical measurements in which all the transition dipole moments from the one-photon allowed states to the one-photon forbidden states can be observed.

As for the CT gap-energy dependence of $\chi^{(3)}$ values, seen in both 1D and 2D cuprates, there could be two possible reasons. One is associated with magnitudes of the nonresonant terms in the denominator of Eq. (2). For instance, in smaller gap materials, the two-photon resonant and the one-photon resonant terms [the second and the third brackets in the denominators of Eq. (2), respectively] are smaller at the three-photon resonant energy. The small nonresonant energy denominators enhance the maximum values of $\chi^{(3)}$. This behavior is generally seen in conventional semiconductors and conjugated polymers. Another possible origin of the CT-gap-energy dependence of $\chi^{(3)}$ is the change in magnitude of transition dipole moments, in the numerators of Eq. (2). Square of the transition dipole moments between the ground state and the one-photon allowed state that dominates the magnitude of the oscillator strength obtained from linear optical measurements is expected to be proportional to $(T_{pd}/\Delta)^2$ (Ref. 14). Here, T_{pd} and Δ represent nearest-neighbor transfer energy and the energy gap between Cu 3d and O 2p one-hole levels, respectively. It has been demonstrated in the 2D cuprates that the oscillator strength increases with decrease of the CT gap energy.¹⁴ Namely, the magnitudes of the transition dipole moments between the ground state and the one-photon allowed state are dominated mainly by Δ . Because the $\chi^{(3)}$ is proportional to the square of the dipole moments, the small CT gap for the small Δ leads to the large $\chi^{(3)}$. Thus, the gap energy dependence of $\chi^{(3)}$, observed experimentally, is attributable to the contributions of the resonant denominators and the transition dipole moments in Eq. (2).

Figure 4(b) shows the Cu-O length dependence of the $\chi^{(3)}$ values, which gives a useful information for us to design good nonlinear optical materials. Both in 1D and 2D cuprates, the $\chi^{(3)}$ values increase with the increase of Cu-O length. This behavior can be easily understood by the fact that the $\chi^{(3)}$ values are dependent on the gap energy, as

discussed above, and that the increase of Cu-O length leads to the decrease of the gap energy through the decrease of the difference (ΔM) in Madelung potential energy M between Cu and O sites.¹⁹ Such a mechanism for the Cu-O length dependence of the gap energy reported for 2D cuprates will stand for 1D cuprates.

In conclusion, we have measured full $\chi^{(3)}$ spectra of La_2CuO_4 and Nd_2CuO_4 by THG. $|\chi^{(3)}|$ spectra were found to exhibit broad peaks due to three-photon resonance of odd CT states in both materials. The $\chi^{(3)}$ phase spectrum of Nd_2CuO_4 reveals that two-photon resonance of the even CT state is hidden on the high-energy side of the $\chi^{(3)}$ peak.

Maximum values of $\chi^{(3)}$ are 0.6×10^{-10} esu in La_2CuO_4 and 2×10^{-10} esu in Nd_2CuO_4 , which are one order of magnitude smaller than those in 1D cuprates, Sr_2CuO_3 and Ca_2CuO_3 . These results are consistent with the results of recent theoretical studies in which coupling or decoupling of spin and charge degrees of freedom and differences in the charge configurations of 1D and 2D cuprates are taken into account.

The authors thank Professors T. Tohyama and S. Maekawa for enlightening discussions. This work was supported by a Grant-In-Aid from the Ministry of Education, Science, Sports and Culture of Japan.

-
- ¹H. Kishida, H. Matsuzaki, H. Okamoto, T. Manabe, M. Yamashita, Y. Taguchi, and Y. Tokura, *Nature (London)* **405**, 929 (2000).
- ²H. Kishida, M. Ono, K. Miura, H. Okamoto, M. Izumi, T. Manako, M. Kawasaki, Y. Taguchi, Y. Tokura, T. Tohyama, K. Tsutsui, and S. Maekawa, *Phys. Rev. Lett.* **87**, 177401 (2001).
- ³T. Ogasawara, M. Ashida, N. Motoyama, H. Eisaki, S. Uchida, Y. Tokura, H. Ghosh, A. Shukla, S. Mazumdar, and M. Kuwata-Gonokami, *Phys. Rev. Lett.* **85**, 2204 (2000).
- ⁴M. Ashida, T. Ogasawara, Y. Tokura, S. Uchida, S. Mazumdar, and M. Kuwata-Gonokami, *Appl. Phys. Lett.* **78**, 2831 (2001).
- ⁵Y. Mizuno, K. Tsutsui, T. Tohyama, and S. Maekawa, *Phys. Rev. B* **62**, R4769 (2000).
- ⁶M. Takahashi, T. Tohyama, and S. Maekawa, *Phys. Rev. B* **66**, 125102 (2002).
- ⁷A. Schülzgen, Y. Kawabe, E. Hanamura, A. Yamanaka, P.-A. Blanche, J. Lee, H. Sato, M. Naito, N.T. Dan, S. Uchida, Y. Tanabe, and N. Peyghambarian, *Phys. Rev. Lett.* **86**, 3164 (2001).
- ⁸A.B. Schumacher, J.S. Dodge, M.A. Carnahan, R.A. Kaindl, D.S. Chemla, and L.L. Miller, *Phys. Rev. Lett.* **87**, 127006 (2001).
- ⁹F. Kajzar, J. Messier, and C. Rosilio, *J. Appl. Phys.* **60**, 3040 (1986).
- ¹⁰R.C. Miller, *Appl. Phys. Lett.* **5**, 17 (1964).
- ¹¹C.G.B. Garrett and F.N.H. Robinson, *IEEE J. Quantum Electron.* **QE-2**, 328 (1966).
- ¹²B. Buchalter and G.R. Merredith, *Appl. Opt.* **21**, 3221 (1982).
- ¹³T. Hasegawa, Y. Iwasa, T. Koda, H. Kishida, Y. Tokura, S. Wada, H. Tashiro, H. Tachibana, M. Matsumoto, and R.D. Miller, in *Light Emission from Novel Silicon Materials*, edited by Y. Kanemitsu, M. Kondo, and K. Takeda [*J. Phys. Soc. Jpn.* **63**, 64 (1994)].
- ¹⁴Y. Tokura, S. Koshihara, T. Arima, H. Takagi, S. Ishibashi, T. Ido, and S. Uchida, *Phys. Rev. B* **41**, 11 657 (1990).
- ¹⁵P.N. Butcher and D. Cotter, *The Elements of Nonlinear Optics* (Cambridge University Press, Cambridge, 1990).
- ¹⁶J.P. Falck, A. Levy, M.A. Kastner, and R.J. Birgeneau, *Phys. Rev. Lett.* **69**, 1109 (1992).
- ¹⁷T. Thio, R.J. Birgeneau, A. Cassanho, and M.A. Kastner, *Phys. Rev. B* **42**, 10 800 (1990).
- ¹⁸M. Ashida, Y. Taguchi, Y. Tokura, R.T. Clay, S. Mazumdar, Yu.P. Svirko, and M. Kuwata-Gonokami, *Europhys. Lett.* **58**, 455 (2002).
- ¹⁹Y. Ohta, T. Tohyama, and S. Maekawa, *Phys. Rev. Lett.* **66**, 1228 (1991).